Final Scientific/Technical Report
DE-FG02-08ER15959
DOE-UCB-15959
University of Colorado
IMAGING OF CONFORMATIONAL CHANGES
Principal Investigator: Josef Michl

1. Executive Summary

Control of intramolecular conformational change in a small number of molecules or even a single one by an application of an outside electric field defined by potentials on nearby metal or dielectric surfaces has potential applications in both 3-D and 2-D nanotechnology. Specifically, the synthesis, characterization, and understanding of designed solids with controlled built-in internal rotational motion of a dipole promises a new class of materials with intrinsic dielectric, ferroelectric, optical and optoelectronic properties not found in nature. Controlled rotational motion is of great interest due to its expected utility in phenomena as diverse as transport, current flow in molecular junctions, diffusion in microfluidic channels, and rotary motion in molecular machines. A direct time-resolved observation of the dynamics of motion on ps or ns time scale in a single molecule would be highly interesting but is also very difficult and has yet to be accomplished. Much can be learned from an easier but still challenging comparison of directly observed initial and final orientational states of a single molecule, which is the basis of this project. The project also impacts the understanding of surface-enhanced Raman spectroscopy (SERS) and single-molecule spectroscopic detection, as well as the synthesis of solid-state materials with tailored properties from designed precursors.

2. Actual Accomplishments vs. Original Objectives

Our ultimate objective is to develop methods for the detection and control of rotary conformational changes in single molecules in real time. In the time period of this report (2008-2015) the research goal was to synthesize a suitable dipolar molecular rotor, mount it on a gold surface, and demonstrate its rotational motion induced by external electrical field by direct observation, using differential barrier height imaging (DBHI) and tip-enhanced resonance Raman spectroscopy (TERS). These objectives have only been met in part, not because of any fundamental obstacles, but because we initially underestimated how much time would be needed, especially for the synthesis, given the resources available.

A suitable dipolar chromophore for use in rotor molecules was synthesized and its transition moment directions determined. Several kinds of rotor molecules were synthesized and mounted on a gold surface. They were observed individually using STM and DBHI, and only one of the polar ones failed to provide evidence that it turns in response to outside electric field. It apparently adopted a surface geometry that made it impossible for the dipole to turn. Possible remedies based on structure modification can be easily proposed, but at this point we ran out of time. The observations were made with a new DBHI/TERS instrument, designed to make correlated maps of Raman band intensities and polarizations for molecules undergoing electric-field induced conformational changes such as rotation. The instrument was built and tested on model samples but only the DBHI functionality was used successfully on actual rotors, due to lack of time.

3. Summary of Activities:

The project involved four types of activities: (i) Design, synthesis, and spectroscopic characterization of chromophores suitable for use in dipolar rotors (2008-2015). (ii) Synthesis of dipolar altitudinal molecular rotors. (2008-2014) (iii) Construction of DBHI/TERS instrumentation for use in the visible part of the spectrum was accomplished in the first funding period (2008-2011) and the extension of the system to the UV in the second funding period (2012-2015). The intended use of the TERS capability in both spectral regimes was for observation of rotation in individual rotor molecules. (iv) Computational work directed at fundamental understanding of the nature of friction in molecular rotors and in molecular machines in general (2008-2012). (v) Computational work towards the finding of suitable metals for extending TERS to the UV (2012-2015).

(i) ***Design, synthesis, and spectroscopic characterization of a carbostyril derivative chromophore for use in altitudinal molecular rotors.*** The initial requirements for suitable chromophores were first, strong visible fluorescence (no dissipative dark processes in the excited state), with absorption and emission both polarized perpendicular to the rotational axis, and second, a large dipole moment, also directed perpendicular to the rotational axis. The number of readily available chromophores that meet these requirements and can serve as rotators is limited. We decided to synthesize a derivative of the laser dye carbostyril for the purpose. We then determined the polarization of its absorption and emission bands and found that it meets the requirements (Fig. 1).

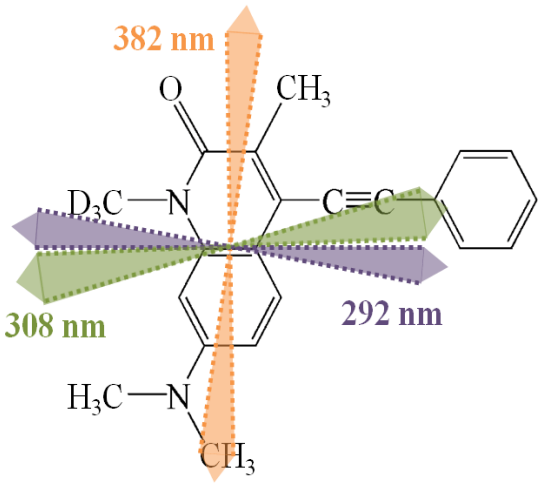

Figure 1. Measured electronic transition moment directions in a carbostyril-based rotator (the triple bond is the axle).

(ii) ***Synthesis of dipolar altitudinal molecular rotors.*** These are fairly complex structures composed of two stands that must adsorb on a gold surface with their direction normal to the surface and are capable of holding an axle that is parallel to the surface and carries a dipolar rotator chromophore, such as carbostyril. The axle has to be located far enough above the surface to permit the rotator to turn freely.

Two types of synthesis of these tailor-made molecular rotors were attempted. The structures shown in Figure 2 were prepared successfully by fairly laborious standard methods of multi-step covalent synthesis. Compounds **1** - **3** were known from our earlier work but had to be made again, while **4** and **5** were new.

The other type of synthesis was non-traditional, a supramolecular metal-ion-directed self-assembly followed by covalent stabilization (Figure 3, which also shows the structure of the carbostyril chromophore in the upper axle). This was a novel, unproven and risky procedure, but it greatly reduces the number of steps and thus removes much of the tedious effort associated with the standard process. It allows a two-step synthesis of complicated structures. The first step is transition-metal-directed self-assembly of ligand-carrying rods into thermodynamically stable entities under equilibrium conditions, and the second step is covalent stabilization that converts the self-

assembled entities into structures that are sturdy enough to be chromatographable.

The ultimate target structure was a two-paddle molecular rotor based on a trigonal prism with differentiated edges (on the right in Figure 3): two edges are functionalized for attachment to a Au(111) surface by a suitable group R, such as a benzylic stannane, and the third acts as an axle for the substituted carbostyril rotor, a chromophore chosen to be in resonance with the TERS excitation beam. Resonance Raman active substituent groups on the chromophore are designed to give signal intensities that will be strongest when the group is aligned by the interaction of the chromophore dipole and the electric field created by the STM tip bias voltage is closest to the tip. They will be weakest when the group is closest to the gold surface. This intensity variation thus provides information about the rotational orientation of the rotator dipole.

We had prior experience with metal-ion directed self-assembly, but the key covalent stabilization step, Pt(+)-N to Pt-C conversion (such as that shown in Figure 3), was unknown and needed to be proven in principle. This was accomplished successfully by the synthesis of simple rectangles. The initial choice of trimethylphosphine as a ligand on Pt failed since it allowed a facile isomerization of the desirable cis isomer into the undesirable trans isomer, thus thwarting the self-assembly. However, a simple remedy was found by using a bridging diphosphine across two phosphine sites and thus preventing the isomerization (Figure 4).

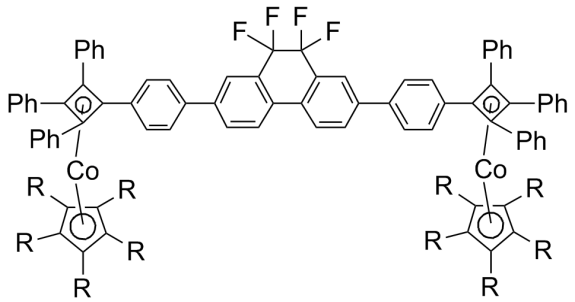

1 R = $HgS(CH_2)_2SCH_3$
2 R = HgO_2CCF_3

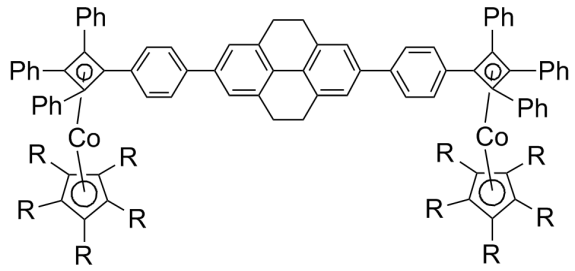

3 R = $HgS(CH_2)_2SCH_3$

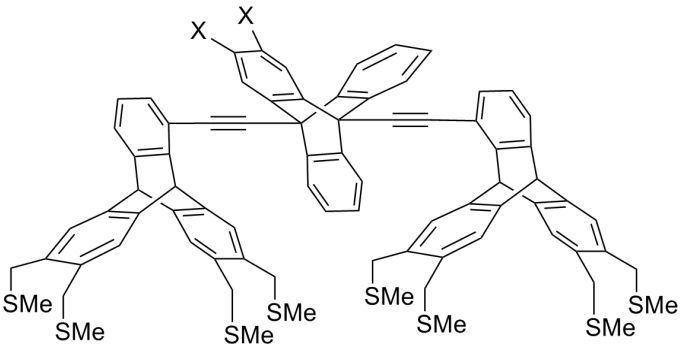

4 X =F
5 X = H

Figure 2. Structures of molecular rotors prepared by traditional covalent synthesis.

A model axial rotor system designed for testing the performance of the TERS instrument was also synthesized. It contained the carbostyril rotator coupled by an axle to three fatty acid chains, suitable for formation of a Langmuir-Blodgett (LB) monolayer (formula **a** in Figure 5). This structure was chosen after a successful preparation of an LB monolayer from a simpler axial rotor with a naphthalene chromophore (formula **b** in Figure 5). The carbostyril compound also formed

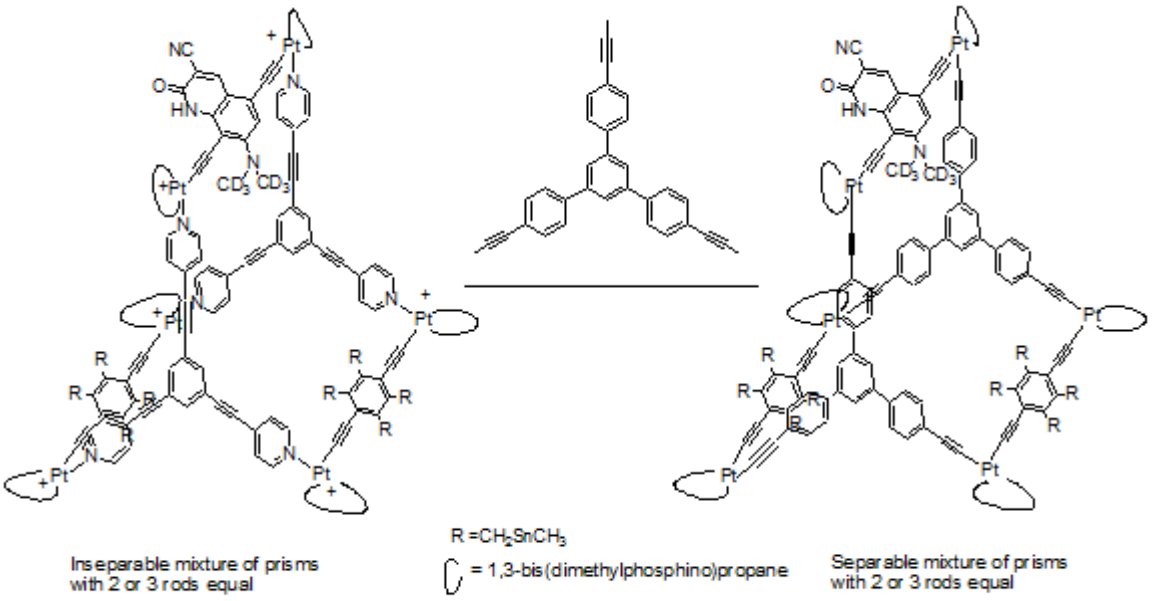

Figure 3. The proposed molecular rotor before (left) and after (right) covalent stabilization. The transformation was to be catalyzed with Cu(I), but it was never attempted.

LB films well. Unfortunately, although it was stable as a solid and in solution, it was destroyed rapidly by photochemical dimerization in the LB film already in ambient light. It appears that in the film the chromophores are packed closely together in an orientation ideal for a 2+2 cycloaddition. In LB films diluted with stearic acid the rotor-carrying molecules segregate into islands and undergo dimerization just as fast. This behavior was fairly unusual and interesting for organic photochemists, but it rendered the compound useless as a model system for testing the performance of the TERS instrument.

(iii) Construction and use of DBHI/TERS instrumentation. We completed an extensive DBHI study on the surface-mounted rotors **1** - **3** shown in Figure 2. Combined with our earlier results on rotors **1** and **3**, we observed altogether three types of surface-mounted rotor behavior: First, dipolar rotors **1** attached to gold through -$HgSCH_2CH_2SCH_3$ groups were shown to reliably respond to a change in the tip polarity about two thirds of time, with some changing their response over a period of about half an hour. Second, rotors **2** attached to gold by -Hg^+ cations were also shown to respond to a change in the tip polarity, but did so more than nine-tenths of time, with little change over long periods of time, suggesting that the occasional blocking of the rotation of **1** is due to interfering alkyl chains. Third, not surprisingly, non-polar rotors **3**, and disappointingly, dipolar rotors **4** attached by -CH_2SCH_3, were invisible in a DBHI scan. The rotational motion in **4** is blocked in some way, presumably as a result of improper side-on binding to the gold surface. It thus appears that the methylthio binding units were a poor choice. We suspect that a modified structure with another binding group would be successful, but did not have time to do the required additional synthetic work.

An illustration of a DBHI scan is provided in Figure 6, which includes an ordinary height-

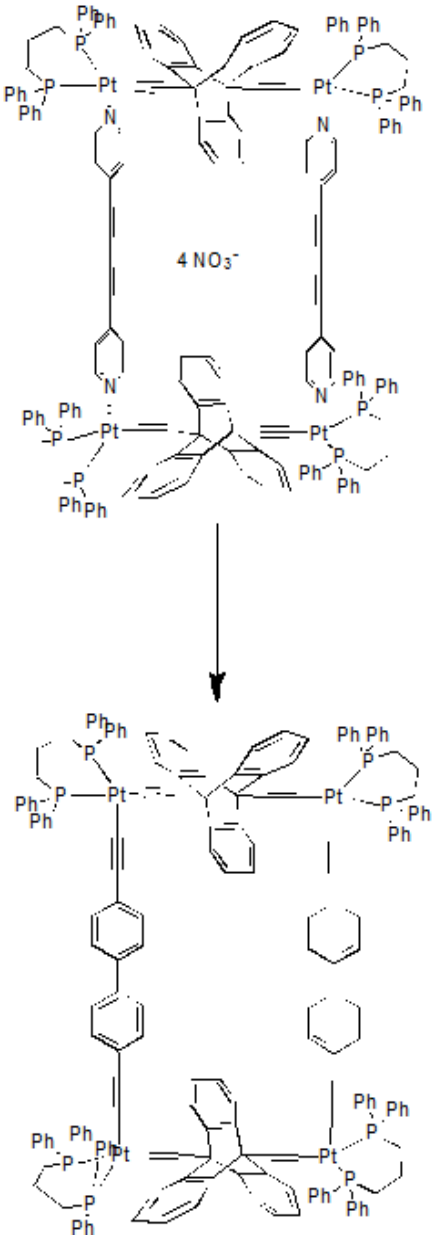

Figure 4. A model system. The achieved covalent stabilization of a self-assembled rectangle, catalyzed by Cu(I).

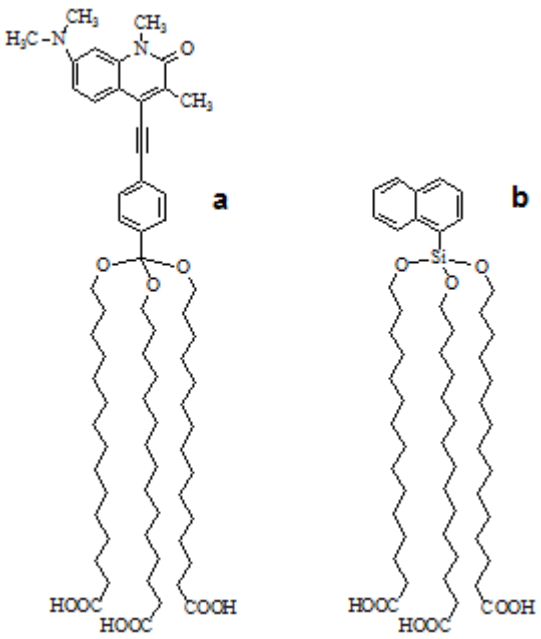

Figure 5. Model axial rotors designed for incorporation in LB monolayers, with carbostyril (**a**) and naphthalene (**b**) rotators.

mode STM image of rotor **4** attached to an Au(111) surface in part (a), two images of the exact same surface region measured simultaneously with a vertically dithered tip used to obtain a map of the work function with the tip biased positively and then negatively during an interleaved scan in parts (c) and (d), and the difference between the latter two scans shown in part (b). The work function difference map shows only those spots where the work function is strongly dependent on the direction of the field, i.e., where the rotors can turn. The system works as it should: the dipole part of the rotor changes its orientation with field direction as the tip is biased from positive to negative, in contrast to step edges which mostly disappear in the difference map since the variation in the local work function in these regions is independent of the field direction.

The proposed combined DBHI/TERS system was built next, first to work in the visible in the first funding period and then upgraded to include near UV in the second funding period. The UV-capable system was tested by exciting a plasmon at the apex of a cobalt STM tip to enhance resonant Raman scattering from a Langmuir-Blodgett film of the commercially available fluorescence marker dye DiA (4-(4(dihexadecylamino)styryl)-N-methylpyridinium iodide). The film was transferred on the downstroke so that the aliphatic chains act as spacer between the chromophore and the gold surface. The Raman spectrum of this film was obtained by excitation of a Co STM tip with 363.8 nm light from an Ar-ion laser (Figure 7). To our knowledge this is the first time UV-TERS has been

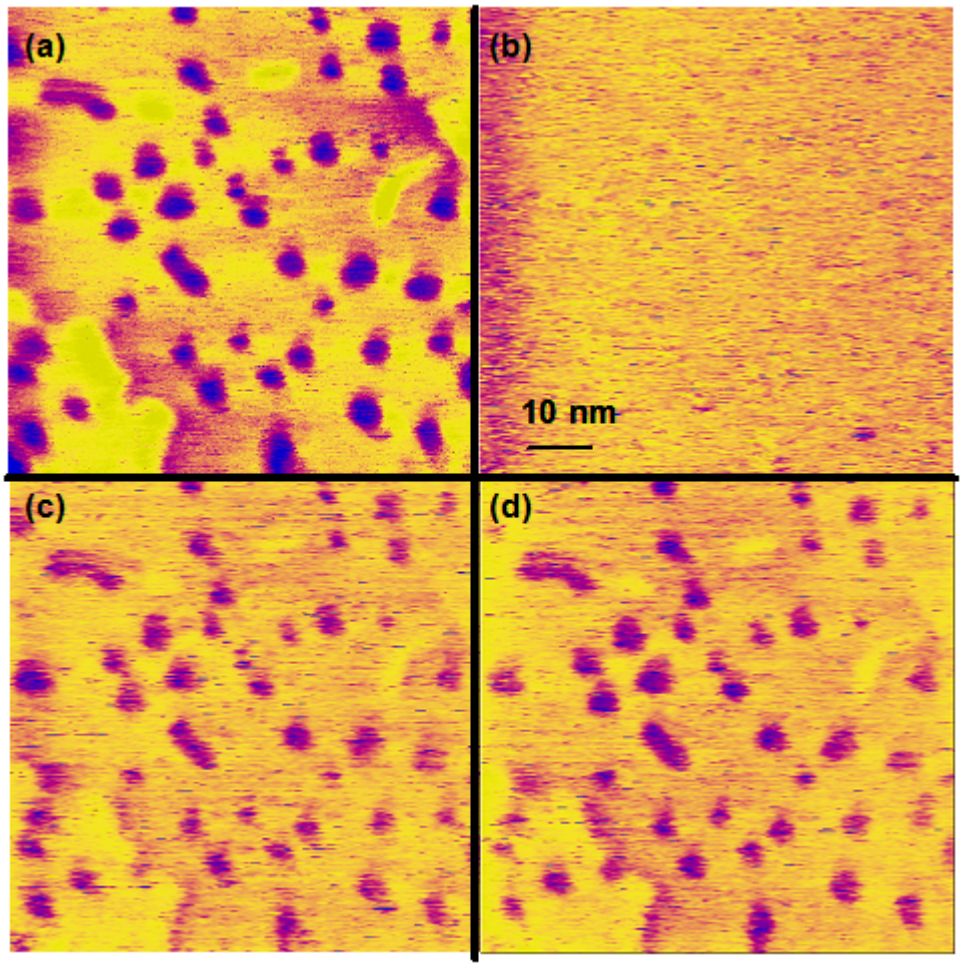

Figure 6. STM (a) and DBHI (b) scans of rotor **4** mounted on gold surface. Panels (c) and (d) show the BHI scans for the two polarities separately.

demonstrated with a cobalt surface plasmon. Cobalt has a broad plasmon resonance calculated near 375 nm (see section 5) that conveniently spans the 363.8 nm line of an Ar-ion laser and one of the strong absorption bands of the carbostyril rotor. The spectrum showed in-plane aromatic bands of the chromophore, but the bands not coupled to the resonant chromophore (methylene bends and stretches of the long-chain aliphatic groups) were invisible.

The DiA dye was rapidly bleached in the laser beam, limiting the collection time to about 60 -130 s and making it hard to obtain high-quality spectra. This should not be a problem for isolated carbostyril rotor molecules but as described above, in the LB films that we prepared they are aggregated, excessively

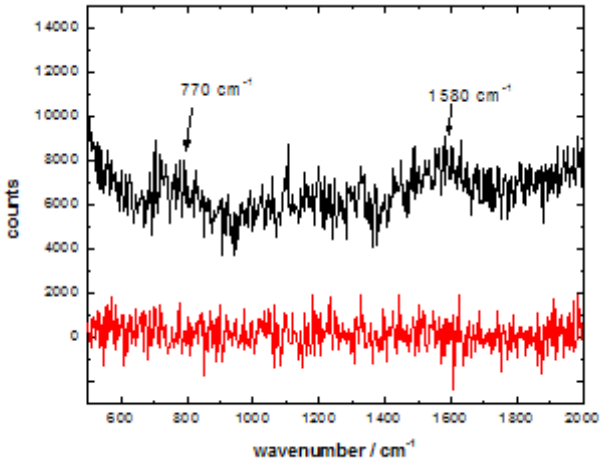

Figure 7. (Black) TERS of DiA at 364 nm with a Co tip. {Red) The same except the tip has been raised 10 nm.

sensitive to light, and could not be used. Since we ran out of time before we were able to prepare carbostyril containing rotors, the ultimately desired DBHI/TERS measurement of a correlated map of the tunneling current, the DBHI plot and the static Raman spectra of single surface-mounted rotor molecules was not accomplished, nor was the collection of dynamic Raman spectra of molecular rotors undergoing rotational conformational changes induced by the tip electric field with the expected 10-ns resolution.

(iv) Computational work. This is described in section 5, Computer Modeling.

4. Products Developed

Publications

Olive, A. G. L.; Parkan, K.; Givelet, C.; Michl, J. "Covalent Stabilization: A Sturdy Molecular Square from Reversible Metal–Ion Directed Self–Assembly", *J. Am. Chem. Soc.* **2011**, *133*, 20108.

Casher, D. L.; Kobr, L.; Michl, J. "Electronic and Vibrational Transition Moment Directions in 7-Dimethylamino-3-methyl-*N*-methyl-d_3-4-phenylethynylcarbostyril", *J. Phys. Chem. A.* **2011**, *115*, 11167.

Casher, D. L.; Kobr, L.; Michl, J. "Average Orientation of a Molecular Rotor Embedded in a Langmuir-Blodgett Monolayer", *Langmuir* **2012**, *28*, 1625.

Prokop, A.; Vacek, J.; Michl, J. "Friction in Molecular Rotors: Classical Molecular Dynamics of Carborane-Based Rotors Driven by Gas Flow or Electric Field", *ACS Nano* **2012**, *6*, 1901.

Two additional papers were submitted for publication but were returned with requests for additional experiments, which we no longer had time to perform.

Technologies/Techniques:

Raman UV-TERS (tip-enhanced Raman spectroscopy in the UV region)/DBHI (differential barrier height imaging) instrument has been built. It uses a cobalt tip (cobalt has a broad plasmon resonance near 375 nm, close to the 361 nm line of the Ar-ion laser and one of the absorption bands of our chromophore, carbostyril. Cobalt has a limited oxide layer and it is well known that it can be etched into sharp STM tips.

5. Computer Modeling

Molecular Dynamics Calculations. The TINK program (Vacek, J.; Michl, J. "A Molecular 'Tinkertoy' Construction Kit: Computer Simulation of Molecular Propellers", *New J. Chem*. **1997**, *21,* 1259.) was used to model the response of dipolar molecular rotors to rotating electric field and to the flow of gas and provided an understanding of the nature of friction in molecular rotors and machines in general as a manifestation of IVR (intramolecular vibrational redistribution). The model is based on molecular mechanics and uses the Universal Force Field for the description of interatomic interactions. The results were published in a peer reviewed journal (*ACS Nano* **2012**, *6*, 1901).

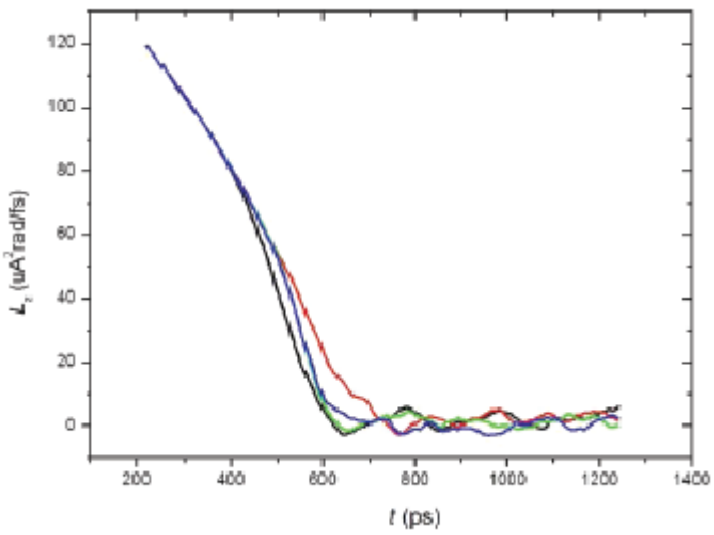

Figure 8. Sample trajectories for loss of rotor angular momentum after the driving electric field has been turned off (free rotation decay), calculated for a representative molecular rotor.

The decay of the rotor rotation rate after the driving electric field is turned off accelerates as the rotor slows (Figure 8), suggesting an inverse relationship between friction and speed at low rates of rotation. The implication of this study for scanning investigations of field-driven rotational conformation change is that the only time dependent signals originate from rotors directly under the force of the driving tip field, since those away from its influence will rapidly stop.

UV Local Surface Plasmon Resonance (LSPR) Calculations. For guidance, the near-field wavelength-dependent EM enhancement $|\boldsymbol{E}|^2$ for a pair of cobalt spheroids was calculated using the discrete dipole scattering approximation implemented using the publicly available DDSCAT programing and methods package. Two identical Co spheroids with a short axis of 40 nm and a 5 : 1 aspect ratio were placed perpendicularly separated by a 1 nm gap and discretized using a mesh of 125000 points. The dielectric constant inside the spheroids was assumed to be uniform and was determined as a function of wavelength by interpolation of tabulated values. Figure 9 shows the electric field intensity $\boldsymbol{E}$ between two Co spheroids

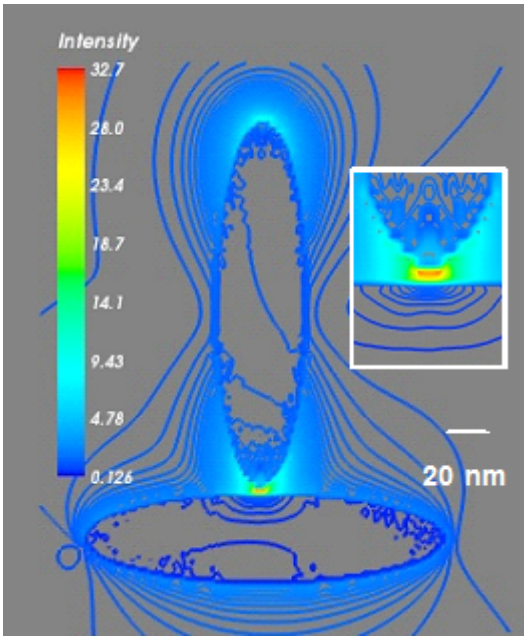

Figure 9. Electric field intensity (arb. units) contours for two Co spheroids relative to the applied electromagnetic field (400 nm: polarized parallel to the long axis of the upper spheroid)

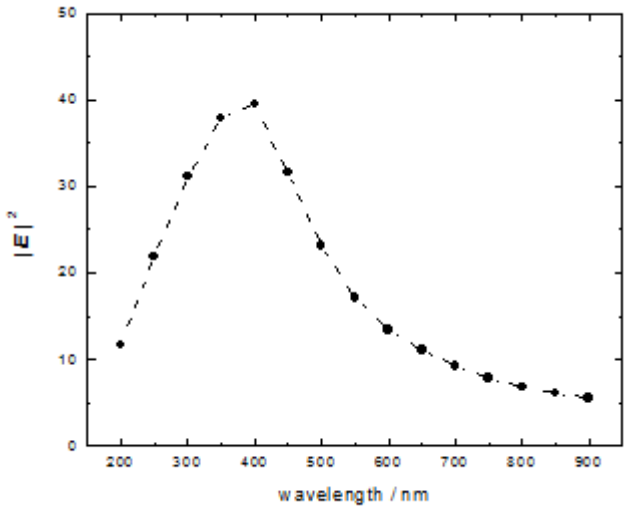

Figure 10. Wavelength dependence of $|\boldsymbol{E}|^2$ (arb. units) for Co spheroids.

whose diameter was chosen to match the typical tip radius of curvature. The value of $\boldsymbol{E}$ is measured relative to the applied field which is nominally assigned a value of unity and is polarized along the *z*-axis of the laboratory frame, parallel to the long axis of the upper spheroid in Figure 9. Figure 10 shows $|\boldsymbol{E}|^2$ as a function of wavelength. The maximum amplitude for the LSPR is at $\lambda_{max} = 400$ nm and agrees with a estimate made from simple Drude theory. The position of the maximum is a function of the aspect ratio of particles and spans a very useful spectral region.